Deep–Sea Research II 173 (2020) 104761

Contents lists available at ScienceDirect

Deep-Sea Research Part II

journal homepage: http://www.elsevier.com/locate/dsr2

Benthic megafauna assemblage change over three decades in the abyss: Variations from species to functional groups

Linda A. Kuhnz [a,b,*], Henry A. Ruhl [a], Christine L. Huffard [a], Kenneth L. Smith [a]

[a] Monterey Bay Aquarium Research Institute, 7700 Sandholdt Road, Moss Landing, CA, 95039, USA
[b] National Oceanography Centre, Southampton, SO14 3ZH, UK

ARTICLE INFO

Keywords:
Deep sea
Benthic
Megafauna
ROV
Pelagic-benthic coupling
Particulate organic carbon
Climate
Time series
California current

ABSTRACT

Megafaunal seafloor assemblages on the Monterey Fan in the NE Pacific (Station M, 4000 m depth) were studied between 2006–2018 using remotely operated vehicles (ROVs) as part of a continuing time-series study that began in 1989. Since 2006 we identified nearly 120,000 individual animals representing over 142 morphospecies, and observed continuous changes in the megafaunal assemblage. This study, which tracked variation in observed morphospecies over a 13-year period, is one of the most detailed long-term records of megafaunal change for abyssal depths. Our investigation shows that new variations continued to emerge, reinforcing the concept that the deep-sea is dynamic over short time scales, rather than static over long periods. Some species were uncommon, but later observed in high numbers, then decreased to very low or undetectable levels (e.g. *Elpidia* sp. A), while others (e.g. *Psychropotes longicauda*) exhibited a relatively persistent presence with less fluctuation in abundance. Decreasing total echinoderm density from 2013–2018 did not correspond with the continued occurrence of large episodic POC flux events between 2016–2018. This may be attributed to the quality of food supply arriving at the seafloor and the varied ability of organisms to utilize it. Long-term tracking (30 years) of 10 specific epibenthic echinoderm species originally quantified from camera-sled images shows a pattern of assemblage structure, perhaps returning toward the composition observed in the 1990s and early 2000s. Many questions remain as to how this abyssal site and others will change with continued, and potentially increasing, anthropogenic change in the upper ocean. For example, the marine heat anomaly known as the 'Warm Blob' may have influenced major ecological processes at the abyssal seafloor in terms of morphospecies and functional group composition due to changes in POC flux. The degree of dynamism continues to indicate that ad hoc or short-term investigations provide a limited perspective for assessing community structure in conservation or resource exploitation impact assessment studies in the deep sea.

1. Introduction

The deep sea was once thought to be a homogenous habitat and relatively unchanging, but is now considered a dynamic ecosystem subject to large changes from natural and anthropogenic-induced influences (Bett et al., 2001; Billett et al., 2001, 2010; Kuhnz et al., 2014; Meyer et al., 2013; Morris et al., 2016; Ruhl and Smith, 2004; Sherman and Smith, 2009; Smith et al., 2002; Taylor et al., 2018). Increased temperatures, ocean acidification, the accumulation of new physical structures (cables, trash), pollution, organic enrichment, mineral mining, and increased noise are altering deep sea ecosystems (Barry et al., 2013; Galley et al., 2008; Paull et al., 2002; Ramirez-Llodra et al., 2011, 2010; Rogers, 2015; Schlining et al., 2013; Smith et al., 2009; Sweetman et al., 2017).

Multiple factors control the structure and composition of deep-sea organismal communities; episodic variations in the quantity and quality of particulate organic carbon (POC) can result in major changes in the density of dominant taxa and community structure. Long-term studies in abyssal areas have helped reveal how such change can occur. Investigations at Station M in the Northeast Pacific Ocean began in 1989 and are ongoing (Huffard et al., 2016; Kuhnz et al., 2014; Ruhl, 2007; Smith et al., 1998, 2006, 2018). Other sustained investigations at the deep seafloor include Porcupine Abyssal Plain (NE Atlantic, PAP, 48°50' N, 16°30' W, Bett et al., 2001, Billett et al., 2001, 2010; Morris et al., 2016) and the Atlantic Ocean and Fram Strait in the Arctic (78°0' N, 0°0' W) (Meyer et al., 2013; Taylor et al., 2018, 2017, 2016).

* Corresponding author.
E-mail address: lkuhnz@mbari.org (L.A. Kuhnz).

https://doi.org/10.1016/j.dsr2.2020.104761
Received 3 September 2019; Received in revised form 17 February 2020; Accepted 17 February 2020
Available online 20 February 2020

The fluctuation of food supply influences deep-sea communities by altering food web structure, organism abundance, and diversity of megafauna (Smith and Druffel, 1998; Smith et al., 2002, 2009; Wigham et al., 2003; Ruhl and Smith, 2004; Ruhl, 2008; Billett et al., 2010; Tecchio et al., 2013). Similar changes have also been observed for macro- and meio-fauna (Gambi and Danovaro, 2006; Laguionie--Marchais et al., 2013), with the responses of microbes being less clear (e.g. Laguionie-Marchais et al., this volume; Rex et al., 2006). These changes have been linked to both direct and indirect evidence of food quality and quantity influencing reproduction and recruitment (Wigham et al., 2003; Ruhl, 2007; FitzGeorge-Balfour et al., 2010). Time-series records have revealed that major portions of the long-term food supply can arrive over periods of weeks or months (e.g. Dunlop et al., 2017; Lampitt et al., 2010; Smith et al., 2018, this volume). However, the longer-term effects of abnormally large POC fluxes to the abyssal seafloor (and periods without such arrivals) on megafauna and community composition remain largely undetermined (Kuhnz et al., 2014).

Here we analyzed data from Station M in the northeast Pacific (Fig. 1). Situated beneath the California Current, Station M is located at the base of the Monterey Canyon abyssal fan at *ca.* 4000 m depth, where seasonal upwelling events lead to pulses of primary production (Smith and Druffel, 1998). These pulses have been shown to affect the megafaunal community at Station M over time (Kuhnz et al., 2014). Additional data bring the long-term monitoring of 10 epibenthic echinoderms to a 30-year time series, allowing us to examine variation from annual to decadal time scales for a limited selection of the megafauna. ROV investigations began in 2006, and are now extended through 2018, which document changes in the entire observed megabenthos assemblage over a 13-year period.

Our aims were to: 1) investigate recent changes in megafaunal assemblage structure in terms of density, diversity and functional group composition from 2013–2018, then combine these six additional years of data with our 2006–2012 results (Kuhnz et al., 2014) to evaluate if previous trends in abundance and diversity continued; 2) examine how changes in the assemblage of 10 epibenthic echinoderms from 2006–2018 relate to observed changes across the observed range of morphospecies and functional groups, i.e. do they follow community trends?; 3) examine the full dataset for possible long-term and potentially cyclical change(s) in the densities and dominance of an assemblage of 10 epibenthic echinoderms studied from 1989–2018, 4) interpret observed community changes in the context of changing climate and particulate organic carbon flux to the seafloor.

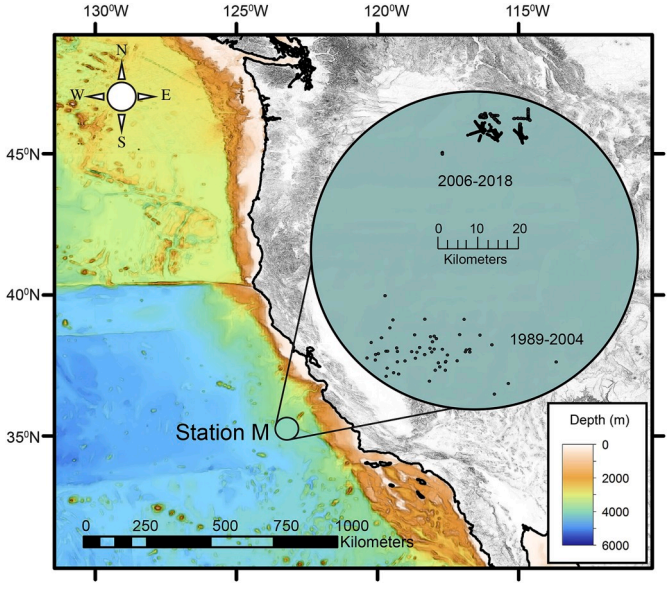

Fig. 1. Map of the western US coast (NE Pacific), showing Station M, 220 km off the California coast. Inset: depiction of areas sampled during this long-term study. Black circles indicate the start point of transects. ROV studies conducted from 2006–2018 are shown to the northeast, while 1989–2004 camera sled sampling took place about 40–50 km to the southwest. Bathymetric layer courtesy of: http://services.arcgisonline.com/ArcGIS/services Ocean_Basemap 2013.

2. Methods

2.1. Surveys

Between 2006–2018, Station M (35°10' N, 122°59' W; Fig. 1) was surveyed 18 times using the Monterey Bay Aquarium Research Institute's (MBARI) R/V *Western Flyer*, equipped with remotely operated vehicles (ROV) *Tiburon* (2006–2007) and *Doc Ricketts* (2009–2018; Fig. 1, Table 1). We conducted video transects within a 40 km^2 area of seafloor at 4000 m depth (± 40 m). Video was recorded with Ikegama high-definition cameras fitted with HA10Xt.2 Fujinon lenses. The ROV was equipped with two parallel laser beams spaced 29 cm apart, which were used to measure a consistent meter-wide strip of the seafloor. ROV transects were typically conducted annually with additional cruises in 2007 (winter, summer, fall), 2011 (spring and winter), 2012 (summer and winter), 2014 (spring and fall), 2015 (summer and winter) and in 2017 (spring and winter, Table 1). Benthic and benthopelagic megafauna (organisms large enough to be identified in seafloor images, about 1 cm in size or larger) were quantified by annotating video footage using MBARI's Video Annotation and Reference System (VARS) (Schlining and Stout, 2006). All species identifications from ROV video were made by one worker (LAK). Care was taken to ensure archived and recent imagery were comparable and that changes in diversity or abundances were not the result of camera or video recording changes over time.

Results of the ROV studies were combined with the earlier time-series data quantified from towed camera-sled images during Station M studies between 1989–2004 for 10 epibenthic echinoderm species.

2.2. Taxonomic and functional group assignment

For the period of 2006–2018, megafauna were identified to the lowest practical taxonomic level. Because the identification of

Table 1
Quantitative transects included in data analysis. For ROV dive number, T indicates ROV *Tiburon* and D for ROV *Doc Ricketts*. We observed substantial detritus on the seafloor during the periods indicated.

Year	Date	ROV Dive	Transect area (m^2)
2006	Dec	T1067	1120
2007	Feb	T1077, 1080	220
2007	June	*T1094	80
2007	Sept	*T1141, 1143	420
2009	Feb	D008	1560
2011	May	D230, 231, 232	4500
2011	Nov	D321, 323, 324	2640
2012	June	$^{+}$D403	400
2012	Nov	*D442, 443	2600
2013	June	D486, 487	2413
2014	April	*D579, 580, 581	2600
2014	Oct	$^{+}$◆D671, 673, 674	2590
2015	June	D772, 774	2680
2015	Nov	D817, 819	1850
2016	Nov	*D902, 903, 904	2730
2017	Mar	*◆D935, 936	2204
2017	Nov	*D983, 986, 987	2338
2018	April	D1016, 1017	1565

* phytodetrital aggregates present $^{+}$dead/dying pelagic salps present.
◆ dead/dying pelagic pyrosomes present.
Note that information in gray indicates dives that were reported in our initial analysis (Kuhnz et al., 2014), but are included in the current analysis for long-term context.

organisms on video can be uncertain, we were conservative in the assignment of taxonomic names. When feasible, specimens were collected to confirm identification. Observed morphospecies were assigned a mobility category (sessile, functionally sessile (can move, but does so infrequently), or mobile) and a feeding-type category (suspension-filter feeder, surface deposit feeder, subsurface deposit feeder, predator/scavenger, or mixed (more than one feeding category applies)). Assignments were based on stable isotope analysis for select abyssal benthic organisms (Iken et al., 2001) with closest congener or group inferences where needed. The assignment of functional categories for each taxon appear in S1.

3. Data analysis

3.1. Benthic megafaunal assemblage (2006–2018)

To examine temporal similarities in species composition over time, we used PRIMER-E v.7 for hierarchical cluster analysis (group average) and non-metric multidimensional scaling analysis (nMDS) based on a Bray Curtis similarity index using square-root-transformed densities. Individual species contributions to the dissimilarity in community composition between years was determined via SIMPER analyses. We also calculated the effective number of species (Hill number analysis), including species richness, the exponential of Shannon's entropy index and the inverse of Simpson's concentration index (Chao et al., 2009, 2014).

3.2. Epibenthic echinoderm assemblage (1989–2018)

The combined dataset analyzed here includes observations from ROV surveys (2006–2018) and the densities of 10 epibenthic echinoderm organisms quantified from towed camera-sled images during previous Station M studies conducted between 1989–2004 (Kuhnz et al., 2014).

Note that better imagery and supplementary specimen sampling since the onset of ROV studies have allowed us to distinguish more species from ROV video than was possible from towed camera images. Refinements to the current morphospecies list have been reconciled with names used in earlier camera sled studies. We combined *Peniagone* sp. A, *P. gracilis*, and *P. papillata* as *Peniagone* sp. A complex for comparison to these historic data; these species were identified as *Peniagone vitrea* in Station M work prior to 2006. *Peniagone* sp. 1 and *Peniagone* sp. 2 were combined as *Peniagone* sp. B complex; these species were identified as *Peniagone diaphana* prior to 2006.

To examine similarities in assemblage composition, we used PRIMER-E v.7 for hierarchical cluster analysis (group average) and non-metric multidimensional scaling analysis (nMDS) based on a Bray Curtis dissimilarity index using square-root-transformed densities for the 10 species tracked for 30 years.

3.3. Climate and particulate organic carbon input to the seafloor

We used data compiled by the Farallon Institute (http://www.farallooninstitute.org, August 2019) referred to as the California Multivariate Ocean Climate Index (MOCI). This index synthesized variation specific to Central California including El Niño Southern Oscillation (ENSO) events, other local and regional atmospheric conditions, and captures information about the timing and strength of the North Pacific marine heat wave, whereby higher than normal sea surface temperatures were detected in 2014–2016 (also known as the 'Warm Blob'). Samples for analyzing particulate organic carbon (POC) flux were collected by sediment trap at 3400 m depth (600 m above bottom (mab)); some data were also used from a trap at 50 mab when the upper trap data were not available. The 50 mab data were adjusted by linear regression to help account for differences arising from relative position in the water column. A time-lapse camera with an oblique field of view recorded images of the seafloor over time, which were used to quantify the percent cover of detrital aggregates and other organic material arriving at the seafloor including detrital salps and pyrosomes. See Smith et al. (2013, 2018) for detailed descriptions of these methods used for quantifying particulate matter inputs at the seafloor. Correlations were examined using the non-parametric Spearman rank correlation (r_s).

4. Results and discussion

4.1. Benthic megafaunal assemblage (2006–2018)

4.1.1. Survey

We quantitatively surveyed an area of seafloor totaling 34510 m^2 of seafloor over 13 years, 2006–2018 (Table 1). Individual transects for the 18 sampling were varied and averaged 1917 m^2. A combined total of nearly 120,000 organisms from 112 morphospecies were quantified, and an additional 30 morphospecies, including benthopelagic fauna were observed in the wider survey area but not quantified on our dive transects (S1).

4.1.2. Data access

The ready availability of data and imagery are important for transparency and long-term assessment at this location and for comparison with other sites (Ardron et al., 2018). Imagery and associated raw annotation and metadata are accessible via MBARI's Deep-Sea Guide at http://dsg.mbari.org/dsg/home, and VARS Public Database Query at https://www.mbari.org/products/research-software/video-annotation-and-reference-system-vars/query-interface/.

4.1.3. Density and dominant organisms

Megafaunal densities ranged from 0.06 ind. m^{-2} in September 2007 to 6.45 ind. m^{-2} in November 2012 (Fig. 2a). Highest density was accentuated by a very dense aggregation of holothurians, which has only been observed once in 30 years. The top ten numerically dominant megafauna in each sampling period accounted for 60.2–83.3% of the total (Table 2). Echinoderms and Porifera (sponges) were numerically dominant in the assemblage (Fig. 2b).

4.1.4. Diversity

The lowest number of morphospecies (species richness) was 23 recorded in June 2007 (Table 3). Sampling periods in 2007 and June 2012 are likely underestimated owing to shorter transect lengths. Species richness remained low through 2009 (30–60 morphospecies), then generally increased to 71–86 thereafter.

The exponential of Shannon's entropy index (Hill 1) reflected that lowest diversity occurred in November 2011 (Table 3, 13.2), and that it continued to be low through October 2014. All dates in 2007 exhibited low diversity as well. Highest diversity (expH' $>$ 20) was observed in November 2018, February 2009, as well as all dates after June 2015 (Table 3). The inverse of Simpson's concentration index (Hill 2) shows a very similar pattern with low diversity in 2007 (13.8–14.6), and high diversity in February 2009 (13.7) and from November 2016–April 2018 (12.5–15.5) (Table 3).

4.1.5. Functional groups

Ongoing changes were reflected in the mobility and trophic levels of megafauna. From 2006–2009, sessile (e.g. sponges, tunicates, anemones), and functionally sessile organisms (e.g. sea pens, brisingid seastars, crinoids) comprised 63–74% of the megafaunal assemblage (Fig. 3a). Thereafter, we observed a major decline in sessile fauna reaching the lowest proportion in June 2013 and comprising only 22% of the megafaunal assemblage. In 2014, the proportion of sessile megafauna gradually increased to more than 50%. Conversely, mobile organisms (e.g. holothurians, ophiuroids) comprised less than a third of the fauna in 2007–2009, then were abundant between 2012–2014 (up to

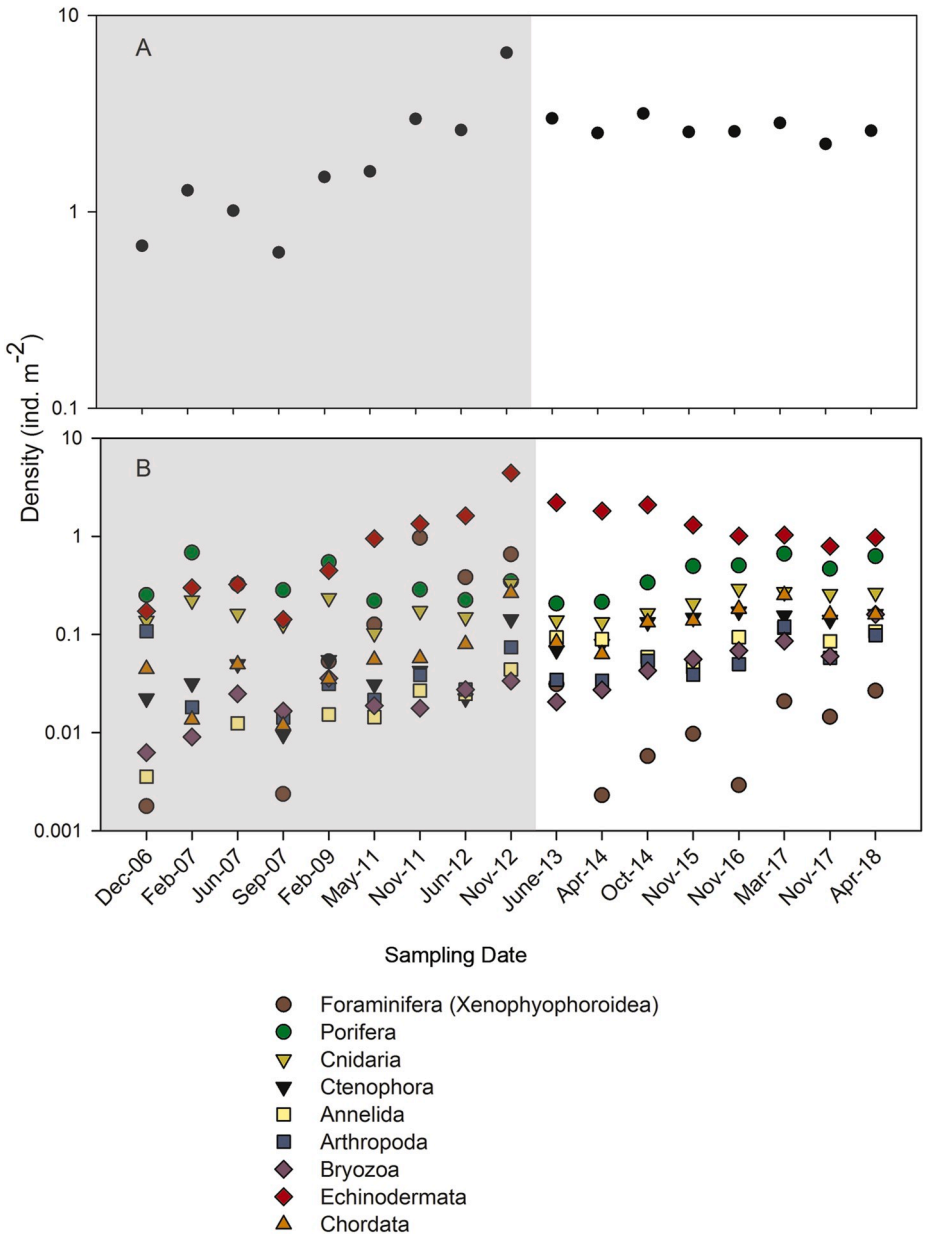

Fig. 2. Sampling period densities (m^2) from 2006–2018; log scales. Densities in the shaded area were previously reported in Kuhnz et al. (2014), and reproduced here for context. A) Total density for organisms observed over 18 ROV sampling periods between 2006–2018. B) Density of organisms for major phylum-level categories.

88% of megafauna). Approximately 50% of the assemblage were sessile taxa over the last four sampling dates (2016–2018).

From 2006–2009, the majority of observed organisms were suspension and filter feeders (62–75%), which included animals such as sponges, tunicates, anemones, zoanthids, and sea pens (Fig. 3b). A persistent, notable drop in the absolute density of suspension and filter feeders occurred in the spring of 2011. Surface deposit feeders (mostly holothurians), subsurface deposit feeders (holothurians, sipunculids), and xenophyophores (mixed feeding strategy) comprised 70–78% of the assemblage from 2011–2014. In mid-2014, suspension and filter feeders began increasing in proportional abundance and leveled off at just over 50% of the megafauna present during the last three sampling periods.

4.1.6. Changes in composition

Between 2011–2012, three species of holothurian (*Peniagone* sp. A, *P. vitrea*-sp. 1 complex, *Scotoplanes globosa*) were observed in very high abundance relative to the early 2000's, but decreased in number after 2015. The holothurians *Peniagone* sp. 2 and *Elpidia* sp. A spiked in abundance for three years each during 2009–2012 and 2011–2013 respectively, but returned to very low, or below detectable densities thereafter. Other holothurians (e.g. *Abyssocucumis abyssorum*, *Benthodytes*, *Benthothuria*, *Oneirophanta mutabilis, Pseudostichous mollis*, *Psychropotes* spp., Synallactidae) exhibited a persistent presence with little, or only brief, fluctuations in density.

Sponge densities also shifted through the time series but somewhat inversely to the holothurians, with fewer individuals observed from 2012–2014, then returning to earlier levels by late 2015 (Fig. 2b). Smaller sponges (<5 cm), many of which were unidentifiable, along with *Bathydorus laevis spinosus*, and the larger plate sponges (*B. laniger* and *Docosaccus maculatus*) accounted for much of this change.

Other taxa became more abundant over time, for example ophiuroids became relatively denser in 2012 and remained so throughout the rest of the time series despite being frequently unobservable (buried or otherwise cryptic), and thus underestimated in abundance. Annelid worms

Table 2
Top 10 dominant morphospecies from Station M ROV surveys for sampling periods 2006–2018. Higher taxonomic group is denoted by (A) Arthropod (B) Bryozoa (C) benthic Ctenophora (Cr) Crinoidea (E) Echinoid (He) Hexacorallia (H) Holothuroidea (O) Ophiuroidea (P) Pennatulacea (Pl) Tube-dwelling polychaeta (Po) Porifera (S) Sipuncula (Si) benthic Siphonophorae (Sc) Scallop (T) Tunicata (X) Xenophyophorae. Gray shading indicates data reported in Kuhnz et al. (2014). Identified SIMPER groups A–G are shown after each sampling date. The top four contributors to specific SIMPER groups are in bold. See S2 for further detail.

December 2006 Group G	mean m-2	% total	February 2007 Group G	mean m-2	% total
Hexactinellida indet. (Po)	0.141	21.0	***Bathydorus laevis pseudospinosus (Po)***	0.277	21.6
Cystechinus loveni (E)	0.065	9.7	**Hexactinellida indet. (Po)**	0.268	20.9
Pennatula sp. indet. (P)	0.046	6.8	Porifera sp. indet. (Po)	0.105	8.1
Epizoanthus stellaris (He)	0.045	6.7	***Cystechinus loveni (E)***	0.086	6.7
Hyalonema bianchoratum (Po)	0.033	4.9	*Epizoanthus stellaris (He)*	0.077	6.0
Cystocrepis setigera (E)	0.030	4.5	*Cystocrepis setigera (E)*	0.068	5.3
Bathydorus laevis pseudospinosus (Po)	0.029	4.3	***Pennatula sp. indet. (P)***	0.059	4.6
Tunicata sp. indet. (T)	0.024	3.6	*Elpidia sp. A (H)*	0.041	3.2
Cladorhiza kensmithi (Po)	0.022	3.3	*Fungiacyathus marenzelle (He)*	0.036	2.8
Tjalfiella (C)	0.021	3.2	*Tjalfiella (C)*	0.032	2.5
Total % attributable to dominants		68.0	Total % attributable to dominants		81.6
June 2007 Group G	**mean m-2**	**% total**	**September 2007 Group G**	**mean m-2**	**% total**
Cystechinus loveni (E)	0.188	19.5	***Bathydorus laevis pseudospinosus (Po)***	0.102	16.5
Bathydorus laevis pseudospinosus (Po)	0.175	18.2	**Hexactinellida indet. (Po)**	0.083	13.4
Pennatula sp. indet. (P)	0.075	7.8	***Cystechinus loveni (E)***	0.071	11.5
Hyalonema bianchoratum (Po)	0.063	6.5	Cladorhiza kensmithi (Po)	0.067	10.7
Tjalfiella (C)	0.050	5.2	***Pennatula sp. indet. (P)***	0.045	7.3
Tunicata sp. indet. (T)	0.050	5.2	*Epizoanthus stellaris (He)*	0.029	4.6
Hexactinellida indet. (Po)	0.050	5.2	*Hyalonema bianchoratum (Po)*	0.024	3.8
Abyssocucumis abyssorum (H)	0.038	3.9	Ophiuroidea spp. (O)	0.021	3.5
Echinocrepis rostrata (E)	0.038	3.9	*Striatodoma dorothea (B)*	0.017	2.7
Epizoanthus stellaris (He)	0.025	2.6	*Echinocrepis rostrata (E)*	0.014	2.3
Total % attributable to dominants		77.9	Total % attributable to dominants		76.3
February 2009 Group G	**mean m-2**	**% total**	**May 2011 Group F**	**mean m-2**	**% total**
Bathydorus laevis pseudospinosus (Po)	0.225	15.0	*Peniagone sp. A (H)*	0.359	22.4
Hexactinellida indet. (Po)	0.178	11.8	*Elpidia sp. A (H)*	0.141	8.8
Cystechinus loveni (E)	0.163	10.8	Ophiuroidea spp. (O)	0.140	8.8

Table 2 (*continued*)

December 2006 Group G	mean m-2	% total	February 2007 Group G	mean m-2	% total
Ophiuroidea spp. (O)	0.108	7.2	Psamminidae sp. indet. (X)	0.126	7.9
Cladorhiza sp. A (Po)	0.090	6.0	*Bathydorus laevis pseudospinosus (Po)*	0.095	5.9
Pennatula sp. indet. (P)	0.055	3.7	*Peniagone sp. indet. (H)*	0.088	5.5
Tjalfiella (C)	0.055	3.7	*Peniagone vitrea (H)*	0.084	5.2
Psamminidae sp. indet. (X)	0.053	3.5	*Scotoplanes globosa (H)*	0.051	3.2
Epizoanthus stellaris (He)	0.047	3.2	Sipuncula sp. indet. (S)	0.044	2.7
Peniagone vitrea (H)	0.044	2.9	Cladorhiza kensmithi (Po)	0.042	2.6
Total % attributable to dominants		67.8	Total % attributable to dominants		72.9
November 2011 Group F	**mean m-2**	**% total**	**June 2012 Group F**	**mean m-2**	**% total**
Psamminidae sp. indet. (X)	0.968	32.6	***Peniagone sp. A (H)***	0.545	20.9
Elpidia sp. A (H)	0.445	15.0	***Elpidia sp. A (H)***	0.465	17.8
Ophiuroidea spp. (O)	0.259	8.7	**Psamminidae sp. indet. (X)**	0.383	14.7
Peniagone sp. A (H)	0.233	7.8	**Ophiuroidea spp. (O)**	0.248	9.5
Peniagone sp. indet. (H)	0.163	5.5	*Scotoplanes globosa (H)*	0.125	4.8
Bathydorus laevis pseudospinosus (Po)	0.117	3.9	*Bathydorus laevis pseudospinosus (Po)*	0.083	3.2
Cladorhiza kensmithi (Po)	0.097	3.3	*Peniagone vitrea (H)*	0.073	2.8
Peniagone vitrea (H)	0.081	2.7	Sipuncula sp. indet. (S)	0.055	2.1
Scotoplanes globosa (H)	0.063	2.1	Cladorhiza kensmithi (Po)	0.053	2.0
?Stephalia dilata (Si)	0.050	1.7	*Peniagone sp. indet. (H)*	0.048	1.8
Total % attributable to dominants		83.3	Total % attributable to dominants		79.6
November 2012 Group E	**mean m-2**	**% total**	**June 2013 Group A**	**mean m-2**	**% total**
Elpidia sp. A (H)	1.335	20.7	***Peniagone sp. A (H)***	0.571	19.1
Ophiuroidea spp. (O)	0.767	11.9	**Ophiuroidea spp. (O)**	0.440	14.7
Peniagone sp. A (H)	0.747	11.6	*Elpidia sp. A (H)*	0.429	14.4
Psamminidae sp. indet. (X)	0.656	10.2	***Scotoplanes globosa (H)***	0.270	9.0
Peniagone sp. 1 (H)	0.626	9.7	*Peniagone vitrea (H)*	0.256	8.6
Scotoplanes globosa (H)	0.289	4.5	*Peniagone sp. indet. (H)*	0.084	2.8
Peniagone vitrea (H)	0.247	3.8	***Bathydorus laevis pseudospinosus (Po)***	0.076	2.5
Tunicata sp. indet. (T)	0.220	3.4	*Tjalfiella (C)*	0.069	2.3
Tjalfiella (C)	0.143	2.2	*Paradiopatra (Pl)*	0.063	2.1
Bathydorus laevis pseudospinosus (Po)	0.135	2.1	Tunicata sp. indet. (T)	0.060	2.0
Total % attributable to dominants		80.0	Total % attributable to dominants		77.6
April 2014 Group A	**mean m-2**	**% total**	**October 2014 Group D**	**mean m-2**	**% total**
Peniagone sp. A (H)	0.760	30.1	***Peniagone sp. A (H)***	0.952	30.1
Ophiuroidea spp. (O)	0.532	21.1	**Ophiuroidea spp. (O)**	0.431	13.6

(*continued on next page*)

Table 2 (*continued*)

December 2006 Group G	mean m-2	% total	February 2007 Group G	mean m-2	% total
Scotoplanes globosa (H)	0.219	8.7	*Peniagone vitrea (H)*	0.371	11.7
Tjalfiella (C)	0.080	3.2	***Tjalfiella (C)***	0.133	4.2
Bathydorus laevis pseudospinosus (Po)	0.075	3.0	*Bathydorus laevis pseudospinosus (Po)*	0.126	4.0
Paradiopatra (Pl)	0.073	2.9	***Scotoplanes globosa (H)***	0.113	3.6
Cladorhiza kensmithi (Po)	0.072	2.9	Cladorhiza kensmithi (Po)	0.100	3.1
Peniagone sp. indet. (H)	0.065	2.6	Tunicata sp. indet. (T)	0.089	2.8
Porifera sp. indet. (Po)	0.048	1.9	Propeamussium meridionale (Sc)	0.065	2.1
Peniagone vitrea (H)	0.046	1.8	Fariometra parvula (Cr)	0.062	2.0
Total % attributable to dominants		78.1	Total % attributable to dominants		77.1
June 2015 Group D	**mean m-2**	**% total**	**November 2015 Group D**	**mean m-2**	**% total**
Peniagone sp. A (H)	0.610	21.0	**Ophiuroidea spp. (O)**	0.481	18.9
Ophiuroidea spp. (O)	0.471	16.2	***Peniagone sp. A (H)***	0.447	17.5
Tjalfiella (C)	0.143	4.9	Porifera sp. indet. (Po)	0.184	7.2
Peniagone vitrea (H)	0.131	4.5	***Tjalfiella (C)***	0.147	5.8
Bathydorus laevis pseudospinosus (Po)	0.122	4.2	Cladorhiza kensmithi (Po)	0.141	5.5
Tunicata sp. indet. (T)	0.114	3.9	*Bathydorus laevis pseudospinosus (Po)*	0.136	5.3
Scotoplanes globosa (H)	0.109	3.7	***Scotoplanes globosa (H)***	0.095	3.7
Porifera sp. indet. (Po)	0.105	3.6	Tunicata sp. indet. (T)	0.090	3.5
Cystocrepis setigera (E)	0.102	3.5	*Cystocrepis setigera (E)*	0.069	2.7
Sipuncula sp. indet. (S)	0.094	3.2	*Cystechinus loveni (E)*	0.064	2.5
Total % attributable to dominants		68.9	Total % attributable to dominants		72.7
November 2016 Group B	**mean m-2**	**% total**	**March 2017 Group B**	**mean m-2**	**% total**
Ophiuroidea spp. (O)	0.589	23.0	*Octacnemidae sp. indet. (T)*	0.715	25.3
Bathydorus laevis pseudospinosus (Po)	0.175	6.9	**Ophiuroidea spp. (O)**	0.510	18.0
Porifera sp. indet. (Po)	0.170	6.6	***Bathydorus laevis pseudospinosus (Po)***	0.302	10.7
Tjalfiella (C)	0.170	6.6	**Porifera sp. indet. (Po)**	0.189	6.7
Tunicata sp. indet. (T)	0.140	5.5	***Tjalfiella (C)***	0.155	5.5
Sipuncula sp. indet. (S)	0.118	4.6	*Peniagone sp. A (H)*	0.137	4.9
Cladorhiza kensmithi (Po)	0.097	3.8	*Scotoplanes globosa (H)*	0.112	3.9
Paradiopatra (Pl)	0.081	3.2	Cladorhiza kensmithi (Po)	0.104	3.7
Scotoplanes globosa (H)	0.079	3.1	*Paradiopatra (Pl)*	0.101	3.6
Cystechinus loveni (E)	0.075	2.9	Munnopsidae (A)	0.093	3.3
Total % attributable to dominants		66.2	Total % attributable to dominants		60.2

Table 2 (*continued*)

December 2006 Group G	mean m-2	% total	February 2007 Group G	mean m-2	% total
November 2017 Group C	**mean m-2**	**% total**	**April 2018 Group C**	**mean m-2**	**% total**
Ophiuroidea spp. (O)	0.417	19.0	**Ophiuroidea spp. (O)**	0.567	21.9
Bathydorus laevis pseudospinosus (Po)	0.178	8.1	**Porifera sp. indet. (Po)**	0.266	10.3
Porifera sp. indet. (Po)	0.139	6.3	***Bathydorus laevis pseudospinosus (Po)***	0.204	7.9
Tjalfiella (C)	0.139	6.3	***Tjalfiella (C)***	0.162	6.2
Sipuncula sp. indet. (S)	0.109	5.0	*Scotoplanes globosa (H)*	0.115	4.4
Cladorhiza kensmithi (Po)	0.104	4.7	Cladorhiza kensmithi (Po)	0.112	4.3
Tunicata sp. indet. (T)	0.096	4.4	*Paradiopatra (Pl)*	0.086	3.3
Scotoplanes globosa (H)	0.089	4.1	Munnopsidae (A)	0.081	3.1
Paradiopatra (Pl)	0.067	3.0	Tunicata sp. indet. (T)	0.070	2.7
Cystechinus loveni (E)	0.064	2.9	*Pennatula sp. indet. (P)*	0.061	2.3
Total % attributable to dominants		63.8	Total % attributable to dominants		66.5

Table 3
Diversity indices (Hill numbers) by sampling date. S = species richness, expH′ = exponential of Shannon's entropy, 1/γ = reciprocal of Simpson's γ

Sampling period	S	expH′	1/γ
December 2006	47	19.1	10.7
February 2007	30	13.8	8.6
June 2007	23	14.6	10.1
September 2007	35	17.7	11.9
February 2009	60	21.5	13.7
May 2011	72	19.7	11.3
November 2011	71	13.2	6.6
June 2012	48	15.5	8.9
November 2012	77	16.3	9.8
June 2013	48	15.5	8.9
April 2014	77	14.3	6.7
October 2014	79	15.9	7.6
June 2015	84	22.4	11.4
November 2015	75	21.1	11.4
November 2016	81	24.6	12.5
March 2017	83	27.3	15.4
November 2017	86	28.1	15.5
April 2018	84	24.2	12.5

(*Paradiopatra*) have gradually increased in abundance over the entire time series as did the bryozoans *Camptoplites* sp. A and *Smithsonius dorothea*.

The most abundant fishes were macrourids in the genus *Coryphaenoides*, which were present in very low density (0–0.007 m^{-2}). The highest fish densities were recorded in 2006–2007, 2014 and 2018. This range was similar to that reported in Drazen et al. (2012), with a new peak abundance over the previous peak of 0.004 ind. m^{-2}.

4.1.7. Community similarity

Ordination, similarity, cluster, and SIMPER analyses (Fig. 4, Table 2) for the megafaunal community revealed three sequential time periods over which the overall assemblage structure changed. Cluster I (2006–2009, Fig. 4, Table 2) reflects the dominant sponges, urchins (*Cystechinus loveni*), and sea pens (*Pennatula)* that were present. The density of other morphospecies e.g. xenophyophores, benthic ctenophores, annelids, bryozoans, and macrourid fishes were observed in very

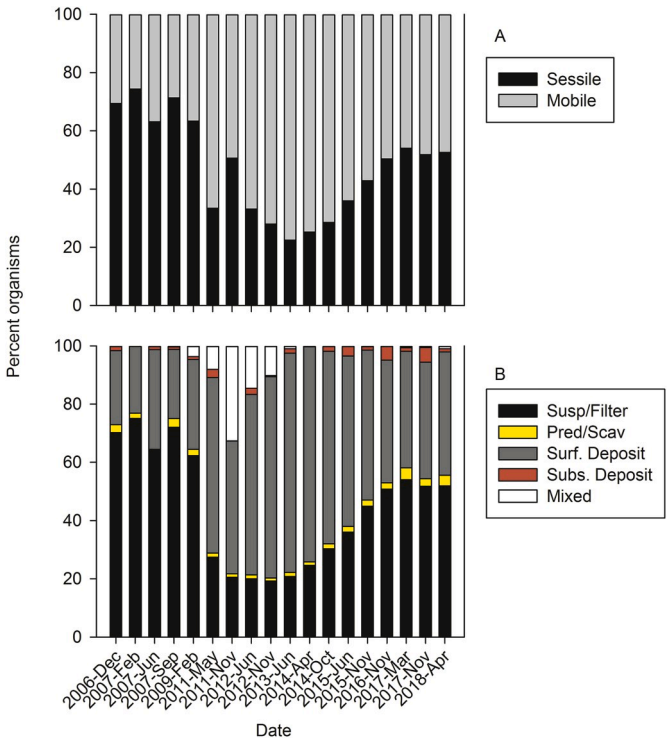

Fig. 3. Functional group analysis. Proportions to the left (2006–2012) were previously reported in Kuhnz et al. (2014), and reproduced here for context. A) Proportion of mobile vs. sessile and functionally sessile organisms over time. Data are based on ROV surveys between 2006–2018. B) Feeding strategies: Suspension feeders, predators and scavengers, surface deposit feeders, subsurface deposit feeders, and mixed category feeders as a proportion of the total from ROV surveys between 2006–2018. Categories after Iken et al., 2001; assignments for each taxa are shown in S1.

low densities during this time. In Cluster II, from 2011–2012 (Fig. 4, Table 2), three dominant holothurians increased in abundance. Ophiuroids also increased, while the densities of other organisms decreased, particularly sponges. Xenophyophores were temporarily observed at nearly an order of magnitude higher than previous or subsequent densities. Benthic ctenophores (*Tjafiella*), the sea pens *Pennatula*, and *Umbellula*, zoanthids *Epizoanthus stellaris*, munnopsid isopod spp., and barnacles (*Verum proximum*) densities initially decreased, but then increased during this time. Cluster III (2013–2018, Fig. 4, Table 2) showed sustained higher abundances for numerous groups of animals. While sponges remained in low density for the first three sampling periods within this cluster, they increased to their previously highest level by 2016. The echinoids, *Cystechinus loveni* and *Cystocrepis setigera*, having been at high density in 2006–2007, regained or surpassed those levels in 2015 after being observed infrequently for 8 years. *E. rostrata* reached its highest density after 2015 as well. *Peniagone* sp. A and *P. vitrea*-sp. 1 complex, and *S. globosa* numbers dropped precipitously in 2016, as did the densities of xenophyophores. *S. globosa*, in contrast to other holothurians, maintained higher than previous densities through 2018.

Continued variation in the megafaunal assemblage at this abyssal site is evident with the inclusion of the additional six years of observations. To date, echinoderms (holothurians, ophiuroids) and sponges are the two most numerically dominant groups in the abyssal seafloor assemblage at Station M over the past 13 years.

As described in Kuhnz et al. (2014), the assemblage changed from a sessile, suspension/filter feeding, sponge-dominated assemblage to a mobile, detritus-feeding holothurian assemblage (the 'Elpidiid Boom') in less than 27 months. That state did not persist; more changes have occurred, and the megafaunal assemblage has not returned to its previous composition. The uniquely large coverage of gelatinous and phytodetrital organic material in 2013 coincided with a large decrease in filter and suspension feeders from a high of 75% (2007) to a low of 22% (2013). Boom and bust cycles of holothurians have been observed previously. In 2002, the species *Amperima rosea* fueled a short-term (<1 year) three orders of magnitude increase in density ("Amperima Event") at the NE Atlantic PAP site (Billett et al., 2010). The holothurians *Kolga*

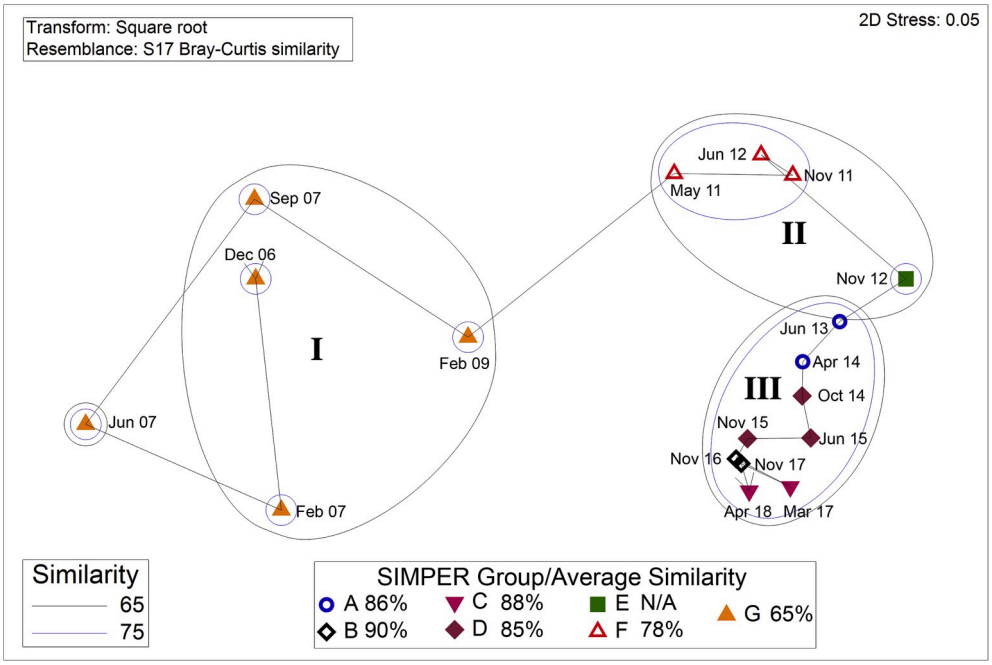

Fig. 4. Multidimensional scaling (MDS) plot for *in situ* morphospecies observed between 2006–2018, with SIMPER groupings shown by symbols. The MDS is based on a Bray Curtis similarity index for square-root transformed densities and similarity is based on hierarchical cluster analysis (single linkage). I, II, and III refer to the three major clusters identified. Average similarity of species contributions are shown next to each SIMPER group (A–G).

hyalina, *Elpidia heckeri* both had large unusual peak abundances in the 2000s at the arctic HAUSGARTEN stations; the timing of these peaks varied by station (Taylor et al., 2018).

4.2. Epibenthic echinoderm subset (1989–2018)

The 10 epibenthic echinoderms show a potential long-term cycle of community similarity when observed over the 30-year dataset. The holothurians *Peniagone* sp. A and *P.* sp. B complex were observed in much lower densities after 2015, and *Elpidia* sp. A was no longer observed on transects after 2014 (Fig. 5). Ophiuroids and the holothurian *S. globosa* have maintained the increased abundance that began in 2012. Holothurians *O. mutabilis*, *Psychropotes longicauda, A. abyssorum*, and Synallactes showed little change in density in the current sampling periods. The echinoid *Echinocrepis rostrata* was observed in slightly higher densities after 2013. The nMDS representation of relative densities reflects the divergence from an initial state in the 1990s, with temporarily higher densities (2001–2002), then moving toward a more depauperate state through the early 2000s and into 2007 (Fig. 6). The high numbers of animals observed in 2011 has gradually decreased though 2018 and similarity for the latter sampling periods may suggest a return to our earliest observed conditions.

4.3. Climate and particulate organic carbon input to the seafloor

Here we found interesting benthic fauna dynamics that warrant further investigation into how the quantity and quality of the sinking particulate food supply is driving ecological change at the seabed. Moreover, these dynamics have occurred in a setting that is experiencing major climatic and oceanographic changes not previously observed during the three decades of observations. For example, the evolution and reoccurrence of the 'Warm Blob' heat anomalies since 2014 have been

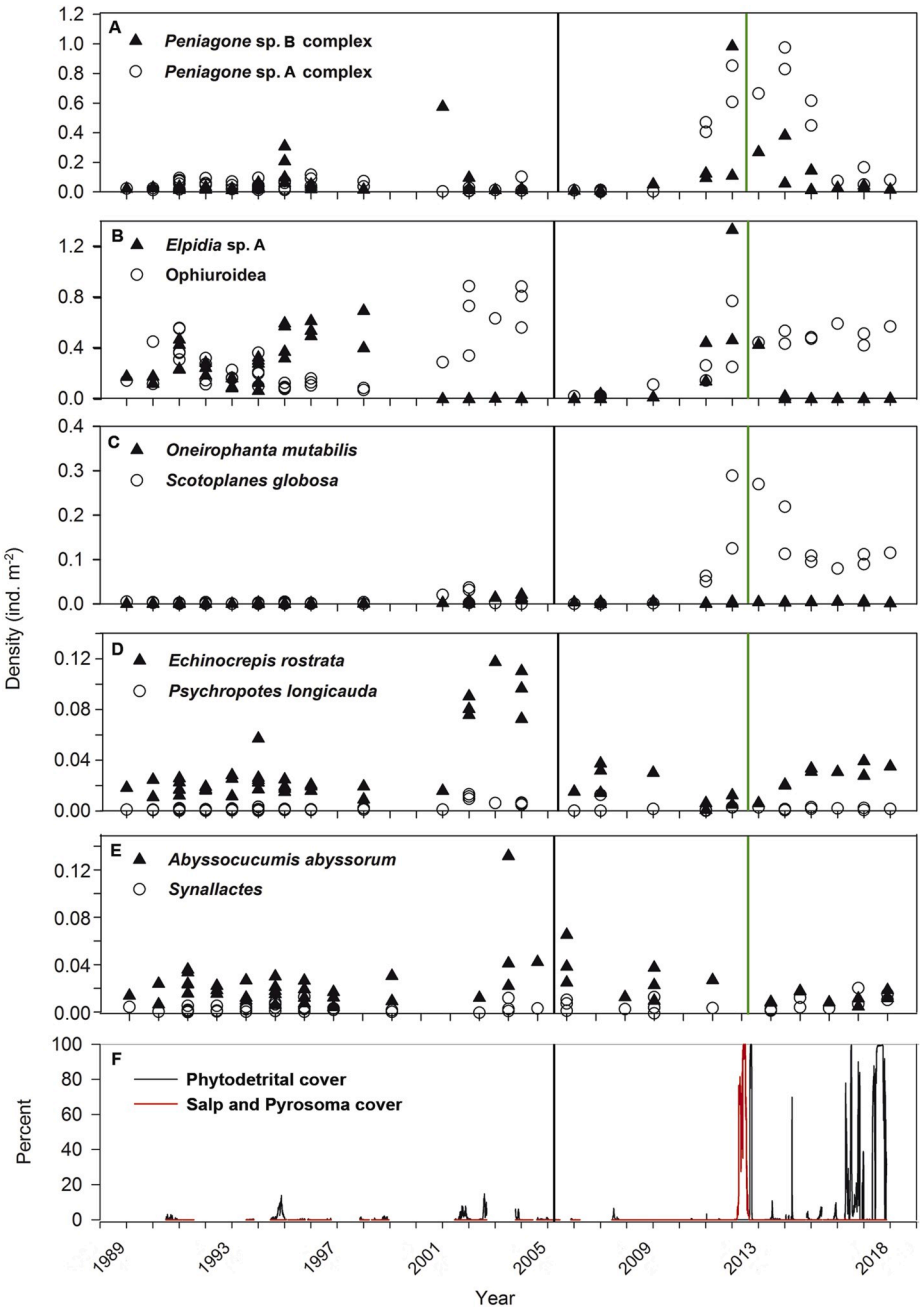

Fig. 5. Densities of ten epibenthic echinoderm species followed from 1989–2018, and the percent cover of potential food falls (phytodetritus, salp detritus, and pyrosome detritus) from time-lapse camera images (after Smith et al., 2018). Sampling dates to the left of the black bar indicate camera-sled sampling, while those after reflect ROV transect data. Green bars indicate current sampling data (2013–2018), while other data have been previously reported in Kuhnz et al. (2014). Note the vertical scale differences in the panels.

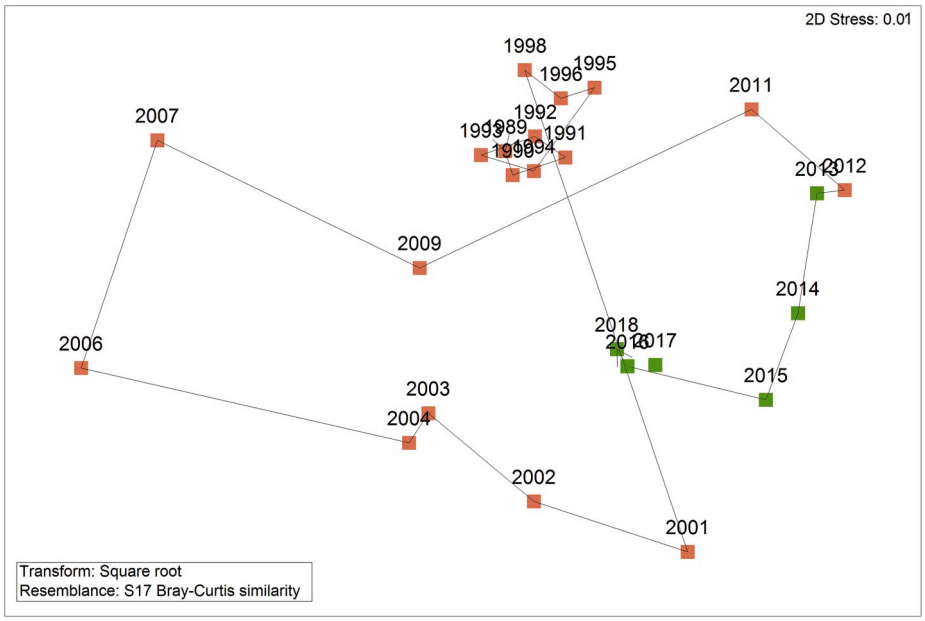

Fig, 6. Multidimensional scaling (MDS) plot for 10 epibenthic echinoderm species followed from 1989–2018. The MDS is based on a Bray Curtis similarity index for square-root transformed densities and similarity is based on hierarchical cluster analysis (single linkage). Orange data points indicate sampling data previously reported in Kuhnz et al. (2014).

linked to large scale changes across the Northeast Pacific (e.g. Bond et al., 2015; García-Reyes and Sydeman, 2017). A regional index of climate and oceanographic change has been created that incorporates variation for offshore Central California that has been attributed to the Warm Blob and related climatic index, the Multivariate Ocean Climate Indicator (MOCI, Sydeman et al., 2014). An initial investigation into potential links between the MOCI index and megafauna assemblage change from 2006–2018 found a significant correlation between the index and the MDS x-ordinate of composition change over time (Fig. 7, Spearman rank correlation, $r_s = 0.68$, $p = 0.002$). However, monthly sediment trap POC flux during this time was not correlated to MOCI or the assemblage composition MDSx during that time. Additionally, there were substantial POC fluxes that were not well observed by the sediment traps, including the episodic deposition of large phytodetritus aggregates and gelatinous material, due to clogging. The potential mechanisms that could produce these large changes in the quantity and quality of food supply to the seafloor at Station M include changes in ocean circulation, primary productivity, ecosystem dynamics and the export flux of POC. While a detailed investigation of the links between food supplies and megafauna assemblage change is beyond the scope of this paper, some observations are suggestive of possible related variations.

It seems probable that such events could have pervasive influences on megafauna assemblages. Large depositions of phytodetrital aggregates were directly observed on the seafloor from ROV footage in June and September of 2007, November 2012, April and October of 2014 (Table 1). They were also present on three consecutive sampling dates between November 2016–2017. A very large pulse of pelagic salp detritus was observed in June 2012, then salp and pyrosome detritus were present on the seafloor in October 2014. Pyrosomes were observed again in March 2017. Importantly, the percent cover of this gelatinous material, based on daily time lapse images through 2017 (Fig. 5F, Smith et al., 2018) approached 100% in 2012 with poorly understood

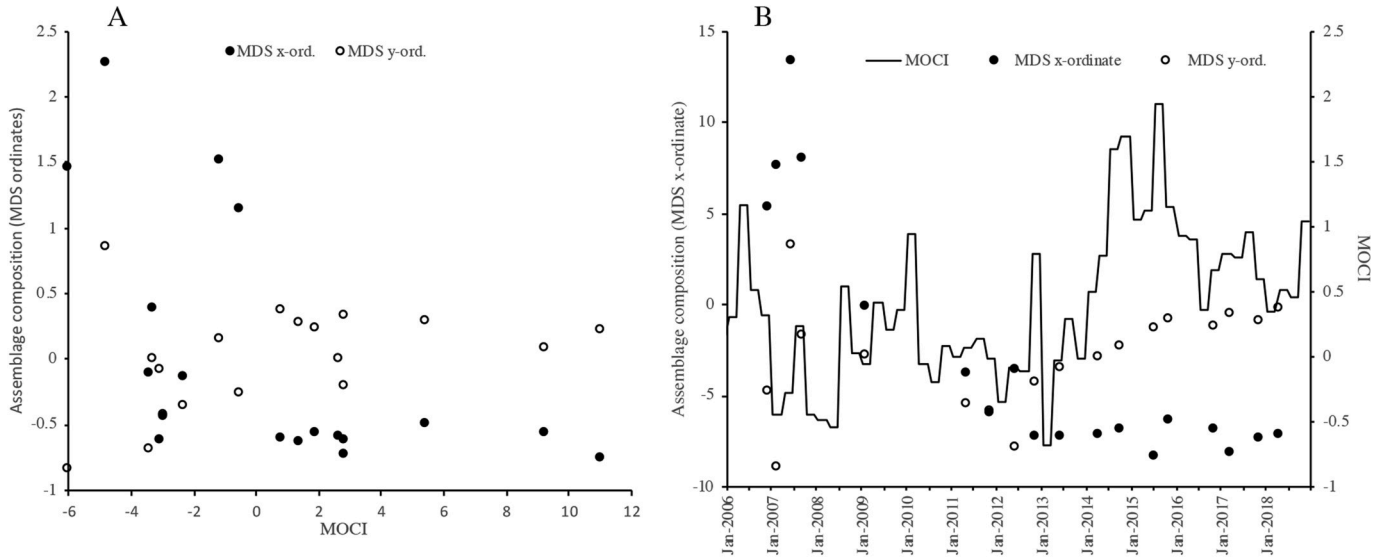

Fig. 7. Initial investigation into potential links between the MOCI index and megafauna assemblage change from 2006–2018.

implications for assemblage change.

Some of the faunal changes we observed correspond to the atypically large increases in food supply (organic carbon) in 2012, which could reach the seafloor from the surface as quickly as 0–70 days (Smith et al., 2018). Large events whereby both gelatinous and phytodetrital material reached the seafloor within a short period make it difficult to understand which influences might have resulted in extremely high densities of holothurians in 2012 (Fig. 5). We also observed a decrease in most holothurian densities after 2013 (*Peniagone* spp. and *Elpidia* sp. A specifically) that do not correspond well to the increasing occurrence of large episodic phytodetritus flux events after 2014–2015. *S. globosa* was an exception as sustained densities after 2012 could indicate that it may respond differently to changes in food supply, and that it was slower to utilize the large pulse of phytodetritus and salps that reached the seafloor in 2012. This idea may be supported by looking at median body length; we found that highest juvenile recruitment for *S. globosa* at Station M occurred between 2011–2014 (Huffard et al., 2016).

It is also important to recognize that some of the observed dynamics may also be explained by body size specific changes in biomass. For example, coherent changes in composition may also be related to greater numbers of small/large individuals with a lower/higher biomass without any change in the overall food supply or density (e.g. Ruhl et al., 2014); biomass estimation was not part of this study.

If the link between the MOCI and the 2006–2018 changes are indeed mechanistic, then food quality may be a key factor. The changing composition of large flux and seafloor cover events and the ability of *S. globosa* to quickly consume multiple food sources may be a factor as well. In an analysis of lipid compositions of holothurians vs. organic matter supply in the western Pacific, Amaro et al. (2019) found that *S. globosa* collected between 4277–5260 m depth contained cholesta-, sitosta- and stigmasta-type sterols and 4ι-methylcholestanol. They concluded that these results were consistent with the direct uptake (deposit-feeding) of fresh phytodetritus. This was contrasted with another species found at Station M, which did not appear to vary in density in response to recent large food input. While *P. longicauda* previously showed a significant positive correlation to the lipids found in surficial sediments (Neto et al., 2006), Amaro et al. found relatively low lipids, but high bacteria levels, indicative of an animal eating more refractory material (2019). They have also been shown to have relatively low chlorophyll a in their gut contents, which may also indicate that they eat more refractory material (FitzGeorge et al., 2010). *P. longicauda* is also one of the largest holothurian species at Station M. Large, slower animals may not have an opportunity to access fresh detritus when in competition with smaller, more active holothurians (Bett et al., 2001).

Large amounts of detritus falling to the seafloor may have a negative impact on some organisms, depending on the composition of it. The conspicuous, sustained drop in abundance of sponges, tunicates, sea pens and other filter/suspension feeders after the heavy salp detritus influx in 2011 may suggest that large amounts of gelatinous material smother or otherwise inhibit these animals. By 2015, the number of filter and suspension feeders increased to their previously higher densities, and those levels have been sustained even though large phytodetrital events have continued.

4.4. Implications for understanding change from human impact

The results here punctuate the need to understand natural variation when looking to detect human impacts on deep-sea animal communities. The detection and monitoring of human impacts to the deep ocean can be accomplished through the availability of reference measures, i.e. baseline data for a study site, and subsequent long-term data, i.e. for detecting potential impact. The study of megafauna as an indicator of baseline conditions is increasing, such as for marine protected areas (e.g. Benoist et al., 2019). Multiple abyssal megafauna studies to understand the ecology of potential seafloor mining areas are revealing high diversity in oligotrophic areas such as the Clarion Clipperton Zone (CCZ, 17°16′N, 122°55′W) (Amon et al., 2016; Gollner et al., 2017; Simon-Lledó et al., 2019). Potential response time scales and effect sizes will need to be considered when designing long-term studies (e.g. Ardron et al., 2019). The prospective impacts range from essentially immediate in the case of seafloor mining (e.g. Durden et al., 2018), interannual to decadal in terms of marine protected areas (e.g. Nickols et al., 2019) and even longer in terms of climate change (e.g. Yool et al., 2017).

5. Conclusions

Change in megafauna community composition and diversity appears to be ongoing at Station M. Results suggest interesting variations that could inform future analyses into detailed links between climate and food supply. The results also punctuate the reality that efforts to monitor the impacts of industrial activity need to include interannual perspectives on change if attribution of impact is to be distinguishable from natural or climate-driven change. Further study may reveal alternate assemblages or thus far unobserved species that exhibit short-term fluctuations that we have missed with our sampling. It may be that the faunal assemblage found in 2015–2018 is indicative of a slow transition back to the 1990s state. Data continue to show that long-term observation is necessary to understand community dynamics, and that thus far we are unable to adequately predict what assemblage state will exist at Station M in the future.

Declaration of competing interest

The authors declare that they have no known competing financial interests or personal relationships that could have appeared to influence the work reported in this paper.

CRediT authorship contribution statement

Linda A. Kuhnz: Methodology, Validation, Formal analysis, Investigation, Data curation, Writing - original draft, Writing - review & editing, Visualization. **Henry A. Ruhl:** Methodology, Formal analysis, Investigation, Writing - review & editing, Visualization. **Christine L. Huffard:** Methodology, Formal analysis, Investigation, Writing - review & editing. **Kenneth L. Smith:** Conceptualization, Methodology, Investigation, Resources, Writing - review & editing, Supervision, Project administration, Funding acquisition.

Acknowledgements

The suggestions and input by our anonymous reviewers have been extremely helpful and we wish to thank them for their time and contributions. We would like to thank the crew of the R/V *Western Flyer* and the *Tiburon* and *Doc Ricketts* ROV pilots. This research was funded by the David and Lucile Packard Foundation (MBARI 901618) and contributes to the California Current Ecosystem - Long-Term Ecological Research (CCE-LTER) program of the National Science Foundation.

Appendix A. Supplementary data

Supplementary data to this article can be found online at https://doi.org/10.1016/j.dsr2.2020.104761.

References

Amaro, T., Danovaro, R., Matsui, Y., Rastelli, E., Wolff, G.A., Nomaki, H., 2019. Possible links between holothurian lipid compositions and differences in organic matter (OM) supply at the western Pacific abyssal plains. Deep-Sea Res. Part I Oceanogr. Res. Pap. 103085. https://doi.org/10.1016/j.dsr.2019.103085.

Amon, D.J., Ziegler, A.F., Dahlgren, T.G., Glover, A.G., Goineau, A., Gooday, A.J., Wiklund, H., Smith, C.R., 2016. Insights into the abundance and diversity of abyssal

megafauna in a polymetallic-nodule region in the eastern Clarion-Clipperton Zone. Sci. Rep. 6, 1–12. https://doi.org/10.1038/srep30492.
Ardron, J.A., Ruhl, H.A., Jones, D.O.B., 2018. Incorporating transparency into the governance of deep-seabed mining in the Area beyond national jurisdiction. Mar. Pol. 89, 58–66. https://doi.org/10.1016/j.marpol.2017.11.021.
Ardron, J.A., Simon-Lledó, E., Jones, D.O.B., Ruhl, H.A., 2019. Detecting the effects of deep-seabed nodule mining: simulations using megafaunal data from the clarion-clipperton zone. Front. Mar. Sci. 6, 604. https://doi.org/10.3389/fmars.2019.00604.
Barry, J.P., Buck, K.R., Lovera, C., Brewer, P.G., Seibel, B.A., Drazen, J.C., Tamburri, M. N., Whaling, P.J., Kuhnz, L., Pane, E., 2013. The response of abyssal organisms to low pH conditions during a series of CO2-release experiments simulating deep-sea carbon sequestration. Deep-Sea Res. Part II Top. Stud. Oceanogr. 1–12. https://doi.org/10.1016/j.dsr2.2013.03.037.
Benoist, N.M.A., Bett, B.J., Morris, K., Ware, S.J., Durden, J.M., LeBas, T.P., Huvenne, V. A.I., Wynn, R.B., Ruhl, H.A., 2019. Monitoring mosaic biotopes in a marine conservation zone by autonomous underwater vehicle. Biol. Conserv. 33 (5), 1174–1186.
Billett, D.S., Bett, B., Rice, A., Thurston, M., Galéron, J., Sibuet, M., Wolff, G., 2001. Long-term change in the megabenthos of the porcupine Abyssal Plain (NE atlantic). Prog. Oceanogr. 50, 325–348. https://doi.org/10.1016/S0079-6611(01)00060-X.
Billett, D.S.M., Bett, B.J., Reid, W.D.K., Boorman, B., Priede, I.G., 2010. Long-term change in the abyssal NE atlantic: the 'Amperima event' revisited. Deep-Sea Res. Part II Top. Stud. Oceanogr. 57, 1406–1417. https://doi.org/10.1016/j.dsr2.2009.02.001.
Bett, B.J., Malzone, M.G., Narayanaswamy, B.E., Wigham, B.D., 2001. Temporal variability in phytodetritus and megabenthic activity at the seabed in the deep Northeast Atlantic. Prog. Oceanogr. 50, 349–368. https://doi.org/10.1016/S0079-6611(01)00066-0.
Bond, N.A., Cronin, M.F., Freeland, H., Mantua, N., 2015. Causes and impacts of the 2014 warm anomaly in the NE Pacific. Geophys. Res. Lett. 42, 3414–3420. https://doi.org/10.1002/2015GL063306.
Chao, A., Colwell, R.K., Lin, C.W., Gotelli, N.J., 2009. Sufficient sampling for asymptotic minimum species richness estimators. Ecology 90, 1125–1133.
Chao, A., Gotelli, N.J., Hsieh, T.C., Sander, E.L., Ma, K.H., Colwell, R.K., Ellison, A.M., 2014. Rarefaction and extrapolation with Hill numbers: a framework for sampling and estimation in species diversity studies. Ecol. Monogr. 84, 45–67. https://doi.org/10.1890/13-0133.1.
Drazen, J.C., Bailey, D.M., Ruhl, H.A., Smith, K.L., 2012. The role of carrion supply in the abundance of deep-water fish off California. PloS One 7, e49332. https://doi.org/10.1371/journal.pone.0049332.
Durden, J.M., Lallier, L.E., Murphy, K., Jaeckel, A., Gjerde, K., Jones, D.O., 2018. Environmental impact assessment process for deep-sea mining in 'the Area'. Mar. Pol. 87, 194–202.
Dunlop, K.M., Jones, D.O.B., Sweetman, A.K., 2017. Direct evidence of an efficient energy transfer pathway from jellyfish carcasses to a commercially important deep-water species. Sci. Rep. 7 (1), 17455. https://doi.org/10.1038/s41598-017-17557-x.
FitzGeorge-Balfour, T., Billett, D.M., Wolff, G.A., 2010. Phytopigments as biomarkers of selectivity in abyssal holothurians, interspecific differences in response to a changing food supply. Deep-Sea Research II 57, 1418–1428.
Galley, E.A., Tyler, P.A., Smith, C.R., Clarke, A., 2008. Reproductive biology of two species of holothurian from the deep-sea order Elasipoda, on the Antarctic continental shelf. Deep-Sea Res. Part II Top. Stud. Oceanogr. 55, 2515–2526. https://doi.org/10.1016/j.dsr2.2008.07.002.
Gambi, C., Danovaro, R., 2006. A multiple-scale analysis of metazoan meiofaunal distribution in the deep Mediterranean Sea. Deep-Sea Res. I 53, 1117–1134.
García-Reyes, M., Sydeman, W.J., 2017. California Multivariate Ocean climate indicator (MOCI) and marine ecosystem dynamics. Ecol. Indicat. 72, 521–529.
Gollner, S., Kaiser, S., Menzel, L., Jones, D.O.B., Brown, A., Mestre, N.C., van Oevelen, D., Menot, L., Colaço, A., Canals, M., Cuvelier, D., Durden, J.M., Gebruk, A., Egho, G.A., Haeckel, M., Marcon, Y., Mevenkamp, L., Morato, T., Pham, C.K., Purser, A., Sanchez-Vidal, A., Vanreusel, A., Vink, A., Martinez Arbizu, P., 2017. Resilience of benthic deep-sea fauna to mining activities. Mar. Environ. Res. 129, 76–101. https://doi.org/10.1016/j.marenvres.2017.04.010.
Huffard, C.L., Kuhnz, L.A., Lemon, L., Sherman, A.D., Smith, K.L., 2016. Demographic indicators of change in a deposit-feeding abyssal holothurian community (station M, 4000m). Deep-Sea Res. Part I Oceanogr. Res. Pap. 109, 27–39. https://doi.org/10.1016/j.dsr.2016.01.002.
Iken, K., Brey, T., Wand, U., Voigt, J., Junghans, P., 2001. Food web structure of the benthic community at the Porcupine Abyssal Plain (NE Atlantic): a stable isotope analysis. Prog. Oceanogr. 50, 383–405. https://doi.org/10.1016/S0079-6611(01)00062-3.
Kuhnz, L.A., Ruhl, H.A., Huffard, C.L., Smith, K.L., 2014. Rapid changes and long-term cycles in the benthic megafaunal community observed over 24 years in the abyssal northeast Pacific. Prog. Oceanogr. 124, 1–11. https://doi.org/10.1016/j.pocean.2014.04.007.
Lampitt, R.S., Billett, D.S.M., Martin, A.P., 2010. The sustained observatory over the Porcupine Abyssal Plain (PAP): insights from time series observations and process studies. Deep-Sea Res. Part II Top. Stud. Oceanogr. 57, 1267–1271. https://doi.org/10.1016/j.dsr2.2010.01.003.
Laguionie-Marchais, C., Billett, D.S.M., Paterson, G.L.D., Ruhl, H.A., Soto, E.H., Smith, K. L., Thatje, S., 2013. Inter-annual dynamics of abyssal polychaete communities in the North east pacific and North east atlantic—a family-level study. Deep-Sea Res. Part I Oceanogr. Res. Pap. 75, 175–186. https://doi.org/10.1016/j.dsr.2012.12.007.
Meyer, K.S., Bergmann, M., Soltwedel, T., 2013. Interannual variation in the epibenthic megafauna at the shallowest station of the HAUSGARTEN observatory (79° N, 6° E). Biogeosciences 10, 3479–3492. https://doi.org/10.5194/bg-10-3479-2013.
Morris, K.J., Bett, B.J., Durden, J.M., Benoist, N.M.A., Huvenne, V.A.I., Jones, D.O.B., Robert, K., Ichino, M.C., Wolff, G.A., Ruhl, H.A., 2016. Landscape-scale spatial heterogeneity in phytodetrital cover and megafauna biomass in the abyss links to modest topographic variation. Sci. Rep. 6 https://doi.org/10.1038/srep34080.
Neto, R.R., Wolff, G.A., Billett, D.S.M., Mackenzie, K.L., Thompson, A., 2006. The influence of changing food supply on the lipid biochemistry of deep-sea holothurians. Deep-Sea Res. Part I Oceanogr. Res. Pap. 53, 516–527. https://doi.org/10.1016/j.dsr.2005.12.001.
Nickols, K., White, J.W., Malone, D., Carr, M.H., Starr, R.M., Baskett, M.L., Hastings L. W., A., Botsford, L.W., 2019. Setting ecological expectations for adaptive management of marine protected areas. J. Appl. Ecol. 56, 2376–2385. https://doi.org/10.1111/1365-2664, 13463.
Paull, C., Greene, H., Ussler, W., Mitts, P., 2002. Pesticides as tracers of sediment transport through Monterey Canyon. Geo Mar. Lett. 22, 121–126. https://doi.org/10.1007/s00367-002-0110-1.
Ramirez-Llodra, E., Brandt, A., Danovaro, R., De Mol, B., Escobar, E., German, C.R., Levin, L.A., Martinez Arbizu, P., Menot, L., Buhl-Mortensen, P., Narayanaswamy, B. E., Smith, C.R., Tittensor, D.P., Tyler, P.A., Vanreusel, A., Vecchione, M., 2010. Deep, diverse and definitely different: unique attributes of the world's largest ecosystem. Biogeosciences 7, 2851–2899. https://doi.org/10.5194/bg-7-2851-2010.
Ramirez-Llodra, E., Tyler, P.A., Baker, M.C., Bergstad, O.A., Clark, M.R., Escobar, E., Levin, L.A., Menot, L., Rowden, A., Smith, C.R., Van Dover, C.L., 2011. Man and the last great wilderness: human impact on the deep sea. PloS One 6, e22588. https://doi.org/10.1371/journal.pone.0022588.
Rogers, A.D., 2015. Environmental change in the deep ocean. Annu. Rev. Environ. Resour. 40, 1–38. https://doi.org/10.1146/annurev-environ-102014-021415.
Rex, M.A., Etter, R.J., Morris, J.S., Crouse, J., McClain, C.R., Johnson, N.A., Stuart, C.T., Deming, J.W., Thies, R., Avery, R., 2006. Global bathymetric patterns of standing stock and body size in the deep-sea benthos. Mar. Ecol. Prog. Ser. 317, 1–8.
Ruhl, H.A., Bett, B.J., Hughes, S.J.M., Alt, C.J.S., Ross, E.J., Lampitt, R.S., Pebody, C.A., Smith, K.L., Smith, Billett, D.S.M., 2014. Links between deep-sea megafauna respiration and community dynamics. Ecology 95, 1651–1662.
Ruhl, H.A., 2008. Community change in the variable resource habitat of the abyssal northeast Pacific. Ecology 89, 991–1000.
Ruhl, H.A., 2007. Abundance and size distribution dynamics of abyssal epibenthic megafauna in the northeast Pacific. Ecology 88, 1250–1262.
Ruhl, H.A., Smith, K.L., 2004. Shifts in deep-sea community structure linked to climate and food supply. Science 305, 513–515. https://doi.org/10.1126/science.1099759.
Schlining, B.M., Stout, N.J., 2006. MBARI's video annotation and reference System. In: Proceedings of the Marine Technology Society/Institute of Electrical and Electronics Engineers Oceans Conference, pp. 1–5.
Schlining, K., von Thun, S., Kuhnz, L., Schlining, B., Lundsten, L., Jacobsen Stout, N., Chaney, L., Connor, J., 2013. Debris in the deep: using a 22-year video annotation database to survey marine litter in Monterey Canyon, central California, USA. Deep-Sea Res. Part I Oceanogr. Res. Pap. 79, 96–105. https://doi.org/10.1016/j.dsr.2013.05.006.
Sherman, A.D., Smith, K.L., 2009. Deep-sea benthic boundary layer communities and food supply: a long-term monitoring strategy. Deep-Sea Res. Part II Top. Stud. Oceanogr. 56, 1754–1762. https://doi.org/10.1016/j.dsr2.2009.05.020.
Simon-Lledó, E., Bett, B.J., Huvenne, V.A.I., Schoening, T., Benoist, N.M.A., Jeffreys, R. M., Durden, J.M., Jones, D.O.B., 2019. Megafaunal variation in the abyssal landscape of the clarion Clipperton zone. Prog. Oceanogr. 170, 119–133. https://doi.org/10.1016/j.pocean.2018.11.003.
Smith, K., Baldwin, R., Karl, D., Boetius, A., 2002. Benthic community responses to pulses in pelagic food supply: North Pacific Subtropical Gyre. Deep-Sea Res. Part I 49, 971–990.
Smith, K., Baldwin, R., Ruhl, H., 2006. Climate effect on food supply to depths greater than 4,000 meters in the northeast Pacific. Limnol. Oceanogr. 51, 166–176.
Smith, K., Druffel, E., 1998. Long time-series monitoring of an abyssal site in the NE Pacific: an introduction. Deep-Sea Res. Part II 45, 573–586.
Smith, K.L., Baldwin, R.J., Glatts, R.C., Kaufmann, R.S., Fisher, E.C., 1998. Detrital aggregates on the sea floor: chemical composition and aerobic decomposition rates at a time-series station in the abyssal NE Pacific. Deep-Sea Res. Part II Top. Stud. Oceanogr. 45, 843–880. https://doi.org/10.1016/S0967-0645(98)00005-8.
Smith, K.L., Ruhl, H.A., Bett, B.J., Billett, D.S.M., Lampitt, R.S., Kaufmann, R.S., 2009. Climate, carbon cycling, and deep-ocean ecosystems. Proc. Natl. Acad. Sci. U.S.A. 106, 19211. https://doi.org/10.1073/pnas.0908322106. –8.
Smith, K.L., Ruhl, H.A., Bett, B.J., Billett, D.S.M., Lampitt, R.S., Kaufmann, R.S., 2013. Climate, carbon cycling, and deep-ocean ecosystems. Proc. Natl. Acad. Sci. U.S.A. 106, 19211–19218. https://doi.org/10.1073/pnas.0908322106.
Smith, K.L., Ruhl, H.A., Huffard, C.L., Messié, M., Kahru, M., 2018. Episodic organic carbon fluxes from surface ocean to abyssal depths during long-term monitoring in NE Pacific. Proc. Natl. Acad. Sci. U.S.A. 115, 12235–12240. https://doi.org/10.1073/pnas.1814559115.
Sydeman, W., Thompson, S.A., García-Reyes, M., Kahru, M., Peterson, W., Largier, J., 2014. Multivariate Ocean-climate indicators (MOCI) for the central California current: environmental change: 2010-2014. Prog. Oceanogr. 120, 352–369.
Sweetman, A.K., Thurber, A.R., Smith, C.R., Levin, L.A., Mora, C., Wei, C., Gooday, A.J., Jones, D.O.B., Rex, M., Yasuhara, M., Ingels, J., Ruhl, H.A., Frieder, C.A., Danovaro, R., Würzberg, L., Baco, A., Grupe, B.M., Pasulka, A., Meyer, K.S., Dunlop, K.M., Henry, L., Roberts, J.M., 2017. Major impacts of climate change on deep-sea benthic ecosystems. Elem. Sci. Anthr. 5 https://doi.org/10.1525/elementa.203.

Taylor, J., Krumpen, T., Soltwedel, T., Gutt, J., Bergmann, M., 2017. Dynamic benthic megafaunal communities: assessing temporal variations in structure, composition and diversity at the Arctic deep-sea observatory HAUSGARTEN between 2004 and 2015. Deep-Sea Res. Part I Oceanogr. Res. Pap. 122, 81–94. https://doi.org/10.1016/j.dsr.2017.02.008.

Taylor, J., Krumpen, T., Soltwedel, T., Gutt, J., Bergmann, M., 2016. Regional- and local-scale variations in benthic megafaunal composition at the Arctic deep-sea observatory HAUSGARTEN. Deep. Res. Part I Oceanogr. Res. Pap. 108, 58–72. https://doi.org/10.1016/j.dsr.2015.12.009.

Taylor, J., Staufenbiel, B., Soltwedel, T., Bergmann, M., 2018. Temporal trends in the biomass of three epibenthic invertebrates from the deep-sea observatory HAUSGARTEN (Fram Strait, Arctic Ocean). Mar. Ecol. Prog. Ser. 602, 15–29. https://doi.org/10.3354/meps12654.

Tecchio, S., Coll, M., Christensen, V., Company, J.B., Ramírez-Llodra, E., Sardà, F., 2013. Food web structure and vulnerability of a deep-sea ecosystem in the NW Mediterranean Sea. Deep-Sea Res. Part I Oceanogr. Res. Pap. 75, 1–15. https://doi.org/10.1016/j.dsr.2013.01.003.

Wigham, B.D., Hudson, I.R., Billett, D.S., Wolff, G.A., 2003. Is long-term change in the abyssal Northeast Atlantic driven by qualitative changes in export flux? Evidence from selective feeding in deep-sea holothurians. Prog. Oceanogr. 59, 409–441. https://doi.org/10.1016/j.pocean.2003.11.003.

Yool, A., Martin, A.P., Anderson, T.R., Bett, B.J., Jones, D.O.B., Ruhl, H.A., 2017. Big in the benthos: future change of seafloor community biomass in a global, body size-resolved model. Global Change Biol. 23, 3554–3566. https://doi.org/10.1111/gcb.13680.